doi:10.1093/brain/aww208 BRAIN 2016: 139; 2641–2652 | 2641

BRAIN
A JOURNAL OF NEUROLOGY

Human cerebrospinal fluid monoclonal *N*-methyl-D-aspartate receptor autoantibodies are sufficient for encephalitis pathogenesis

Jakob Kreye,[1,2,*] Nina K. Wenke,[1,*] Mariya Chayka,[1] Jonas Leubner,[1,2] Rajagopal Murugan,[3,4] Nikolaus Maier,[5] Betty Jurek,[1] Lam-Thanh Ly,[1] Doreen Brandl,[1] Benjamin R. Rost,[1,5] Alexander Stumpf,[5] Paulina Schulz,[1,2] Helena Radbruch,[6,7] Anja E. Hauser,[6,8] Florence Pache,[2,6,8] Andreas Meisel,[2,8,9] Lutz Harms,[2] Friedemann Paul,[2,8,9] Ulrich Dirnagl,[1,2,10] Craig Garner,[1] Dietmar Schmitz,[1,5,11] Hedda Wardemann[3,4] and Harald Prüss,[1,2]

*These authors contributed equally to this work.

See Zekeridou and Lennon (doi:10.1093/aww213) for a scientific commentary on this article.

Anti-*N*-methyl-D-aspartate receptor (NMDAR) encephalitis is a recently discovered autoimmune syndrome associated with psychosis, dyskinesias, and seizures. Little is known about the cerebrospinal fluid autoantibody repertoire. Antibodies against the NR1 subunit of the NMDAR are thought to be pathogenic; however, direct proof is lacking as previous experiments could not distinguish the contribution of further anti-neuronal antibodies. Using single cell cloning of full-length immunoglobulin heavy and light chain genes, we generated a panel of recombinant monoclonal NR1 antibodies from cerebrospinal fluid memory B cells and antibody secreting cells of NMDAR encephalitis patients. Cells typically carried somatically mutated immunoglobulin genes and had undergone class-switching to immunoglobulin G, clonally expanded cells carried identical somatic hypermutation patterns. A fraction of NR1 antibodies were non-mutated, thus resembling 'naturally occurring antibodies' and indicating that tolerance induction against NMDAR was incomplete and somatic hypermutation not essential for functional antibodies. However, only a small percentage of cerebrospinal fluid-derived antibodies reacted against NR1. Instead, nearly all further antibodies bound specifically to diverse brain-expressed epitopes including neuronal surfaces, suggesting that a broad repertoire of antibody-secreting cells enrich in the central nervous system during encephalitis. Our functional data using primary hippocampal neurons indicate that human cerebrospinal fluid-derived monoclonal NR1 antibodies alone are sufficient to cause neuronal surface receptor downregulation and subsequent impairment of NMDAR-mediated currents, thus providing ultimate proof of antibody pathogenicity. The observed formation of immunological memory might be relevant for clinical relapses.

1 German Center for Neurodegenerative Diseases (DZNE) Berlin, Germany
2 Department of Neurology and Experimental Neurology, Charité, Universitätsmedizin Berlin, Germany
3 Max Planck Institute (MPI) for Infection Biology, Berlin, Germany
4 German Cancer Research Center (DKFZ), B Cell Immunology, Heidelberg, Germany
5 Neuroscience Research Center, Charité, Universitätsmedizin Berlin, Germany
6 German Rheumatism Research Centre Berlin (DRFZ), Germany
7 Department of Neuropathology, Charité, Universitätsmedizin Berlin, Germany
8 NeuroCure Clinical Research Center, Charité, Universitätsmedizin Berlin, Germany
9 Experimental and Clinical Research Center, Max Delbrueck Center for Molecular Medicine and Charité Universitätsmedizin Berlin, Germany

Received February 13, 2016. Revised June 9, 2016. Accepted July 5, 2016. Advance Access publication August 20, 2016

10 Center for Stroke Research (CSB) Berlin, Germany
11 Einstein Center for Neurosciences Berlin, Germany

Correspondence to: H. Prüss, MD,
German Center for Neurodegenerative Diseases (DZNE) Berlin,
c/o Charité – Universitätsmedizin Berlin, CharitéCrossOver (CCO),
R 4-334, Charitéplatz 1, 10117 Berlin,
Germany
E-mail: harald.pruess@charite.de

Keywords: NMDA receptor encephalitis; monoclonal auto-antibody; cerebrospinal fluid; electrophysiology; germline antibodies

Abbreviation: NMDAR = *N*-methyl-D-aspartate receptor

Introduction

Discovered only a few years ago, anti-NMDA receptor (NMDAR) encephalitis has become one of the most commonly identified causes of encephalitis and an important differential diagnosis for new-onset psychosis, characteristically associated with hallucinations, catatonia, altered levels of consciousness, seizures, hypoventilation, dyskinesias, and autonomic dysfunction (Dalmau *et al.*, 2007). Despite its often severe course requiring prolonged episodes of intensive care unit treatment and mechanical ventilation, a majority of patients show marked recovery with sufficient immunotherapy (Titulaer *et al.*, 2013). Clinical diagnosis can be established when serum or CSF antibodies bind to the NR1 subunit of the NMDAR, routinely tested with cell-based assays using NR1-transfected human embryonic kidney cells (Peery *et al.*, 2012).

The relevance of a predominantly humoral immune response in NMDAR encephalitis has been concluded from the beneficial effect of plasma exchange, which is widely considered as first-line immunotherapy (Titulaer *et al.*, 2013), and from experiments with human specimen-derived immunoglobulins containing NMDAR antibodies that downregulated NMDAR *in vitro* and *in vivo* (Hughes *et al.*, 2010; Prüss *et al.*, 2010; Mikasova *et al.*, 2012; Moscato *et al.*, 2014; Planaguma *et al.*, 2015). Previous work showed that patients' immunoglobulin contained antibodies that target an epitope in the amino terminal domain of the receptor (Gleichman *et al.*, 2012). However, little is known about which cells produce the antibodies in the CNS, the molecular features of NMDAR autoantibodies, and the frequency of cells producing non-NMDAR binding antibodies in the CSF of patients with NMDAR encephalitis. More importantly, these previous studies could not discriminate between the effect of NMDAR antibodies and the contribution of further anti-neuronal autoantibodies present in CSF. Indeed, diagnostic laboratories commonly identify antibody-binding to brain structures beyond the NR1 immunofluorescence staining pattern, and some clinical features of the disease are not well explained by downregulation of NMDARs, such as susceptibility to epileptic seizures, which has so far been associated with increased or unchanged receptor expression (Kalev-Zylinska *et al.*, 2009; Wasterlain *et al.*, 2013; Wright *et al.*, 2015). Thus, ultimate proof is lacking that NMDAR antibodies alone are sufficient to cause neuronal receptor downregulation and electrophysiological changes associated with the disease.

We therefore aimed to characterize the monoclonal antibody repertoire from CSF antibody-secreting cells and memory B cells of patients with NMDAR encephalitis. In an unbiased approach we generated recombinant monoclonal antibodies by single cell cloning and sequencing of full-length immunoglobulin heavy, kappa and lambda light chain genes. We demonstrate that patients mount a polyclonal antibody response against NMDAR and many further neuronal proteins, and that NMDAR binding of monoclonal recombinant NR1 antibodies generated from patients is sufficient to cause NMDAR downregulation and functional impairment of NMDAR-mediated currents.

Materials and methods

Study approval

All mice were used according to the Berlin LaGeSo Standing Committee on Animals. All clinical investigations were conducted according to Declaration of Helsinki principles. Written informed consent was received from participants at the Charité Department of Neurology or their representatives prior to inclusion in the study and analyses were approved by the Charité University Hospital Institutional Review Board.

CSF single cell isolation

Single cell sorting was performed as previously described (Tiller *et al.*, 2008). In brief, fresh CSF samples were transferred on ice and immediately centrifuged at 400*g* for 10 min. The supernatant was removed and cells resuspended in 500 µl freezing medium [45% RPMI, 45% foetal calf serum, 10% dimethylsulphoxide (DMSO)] and stored at −80°C. For fluorescence-activated cell sorting (FACS) into 96-well PCR plates using a FACSAria™ II (BD Biosciences), frozen cells were thawed, diluted in phosphate-buffered saline (PBS) and stained on ice with antibodies from BioLegend (anti-CD16, 1:50; Zombie Yellow, 1:100), Miltenyi Biotec (anti-CD20, 1:40; anti-CD27, 1:11; anti-CD38, 1:50; anti-IgD, 1:22), and own supply (Flow Cytometry Core Facility, MPIIB) (anti-CD3, 1:100; anti-CD14, 1:50). Each well contained 4 µl of ice-cold lysis solution of 0.5 × PBS with 10 mM DTT (Invitrogen) and 8 U RNasin® (Promega).

Polymerase chain reaction strategy

Single cell reverse transcriptase-polymerase chain reaction (RT-PCR) was performed as previously described (Tiller *et al.*, 2008) in 96-well plates with a volume of 14 µl per sample containing 150 ng random hexamer primer p(dN)$_6$ (Roche), 0.5 µl dNTP-Mix with 25 mM from each nucleotide (Peqlab), 1 µl 0.1 M DTT (Invitrogen), 0.5 µl 10% IGEPAL® CA-630 (Sigma), 14 U RNasin® (Promega) and 50 U SuperScript® III reverse transcriptase (Invitrogen). For the variable immunoglobulin (Ig) gene amplification of immunoglobulin heavy chain (*IGH*) and both possible immunoglobulin light chains (*IGK* and *IGL*) from the cDNA of each well, a nested PCR strategy in two steps was used. PCRs were performed in 96-well plates with 40 µl/well containing 325 nM total primer or primer mix (Supplementary Table 2), 250 nM of each dNTP (Invitrogen) and 0.9 U HotStarTaq® DNA polymerase (Qiagen). cDNAs (2.0 µl) were used as templates for first PCRs, and 3.5 µl of unpurified first PCR product for nested reactions. Each round of PCR was performed at initial 94°C for 15 min, 50 cycles at 94°C for 30 s, 58°C (*IGH*/*IGK*) or 60°C (*IGL*) for 30 s and 72°C for 55 s (first PCR) or 45 s (second PCR) before a final 72°C for 10 min.

Immunoglobulin sequence analysis

The second PCR products were sequenced (GATC Biotech) with reverse primers for *IGH*, *IGK* and *IGL* (Supplementary Table 2). Sequences were compared by IgBLAST with GenBank (http://www.ncbi.nlm.nih.gov/igblast/) to identify germline V(D)J gene segments with highest sequence homology (Corbett *et al.*, 1997). For each immunoglobulin chain sequence the number of somatic hypermutations in the immunoglobulin gene were counted in comparison to the annotated germline sequences as well as the length of the complementarity determining region (CDR3) as described previously (Kabat *et al.*, 1983; Kabat and Wu, 1991).

Cloning into expression vectors

Immunoglobulin gene cloning was performed as previously described (Tiller *et al.*, 2008). Restriction sites were introduced into heavy and light chains for each immunoglobulin (AgeI and SalI for *IGH*, AgeI and BsiWI for *IGK*, AgeI and XhoI for *IGL*) using individual immunoglobulin gene-specific primers (Supplementary Table 2). PCR conditions were as above for the second PCR for heavy chains. Restriction digest was performed at 37°C for 1 h in 40 µl with 31.5 µl of purified specific PCR product and 1 U of each enzyme AgeI, SalI and XhoI (New England Biolabs). Only for *IGK* samples, 1 U of BsiWI enzyme was added and secondarily digested at 55°C for 1 h. Purified products were ligated into expression vectors containing human *IGHG1*, *IGK* and *IGL* constant regions, respectively with a cytomegalovirus (CMV) promotor and ampicillin resistance (Wardemann *et al.*, 2003; Tiller *et al.*, 2008). Ligation product (2.5 µl) was transformed into 6 µl of high efficiency 10-beta competent *Escherichia coli* bacteria (NEB). Positive colonies were screened for inserts (650 bp for *IGHG1*, 700 bp for *IGK* and 590 bp for *IGL*) by PCR (primers as in Supplementary Table 2) and sequenced. In case of 100% identity to the original PCR sequence, plasmid DNA was isolated (NucleoSpin® Plasmid Kit, Macherey and Nagel) from 2 ml of an overnight bacteria culture in Terrific Broth (Gibco Life Technologies) containing 100 µg/ml ampicillin. Plasmid concentration was determined via µDrop™ (ThermoFisher).

Recombinant monoclonal antibodies

Antibody production was performed as previously described (Tiller *et al.*, 2008). In brief, human embryonic kidney (HEK293T) cells were cultured in 6-well plates in Dulbecco's modified Eagle medium (DMEM) supplemented with 10% heat-inactivated foetal bovine serum (FBS), 100 U/ml penicillin, and 100 µg/ml streptomycin (Gibco Life Technologies). At 60–80% confluence, cells were transiently transfected in DMEM supplemented with 1% Nutridoma-SP (Roche), 100 U/ml penicillin, and 100 µg/ml streptomycin with a transfection solution of 75 µl sterile sodium chloride, 0.75 µg HC vector, 0.75 µg LC vector and 7.5 µl polyethylenimine (PEI, 0.6 g/l) solution (Sigma-Aldrich). Supernatant was harvested after 3 and 5 days. Antibody concentration was on average 30 µg/ml ranging from 10 to 80 µg/ml.

Antibody purification

Supernatant was incubated with 2 µl Protein G Sepharose® beads (GE Healthcare) per ml for 1 h at room temperature. Samples were centrifuged at 800*g* for 10 min, the supernatant removed and the beads transferred to a chromatography spin column (Bio-Rad), equilibrated with PBS. After washing the columns twice with 1 ml PBS, antibodies were eluted in two fractions, each with 400 µl elution buffer [0.1 M sodium citrate (pH 2.7), pH-neutralized with 40 µl 1 M Tris (pH 8.8)] per tube and dialysed overnight with PBS. IgG concentrations were determined with ELISA according to the manufacturer's instructions (Mabtech).

Screening for NR1 reactivity

HEK293T cells were transiently transfected with NR1 DNA (1 µg) as described (Prüss *et al.*, 2015). Two days later, HEK cells on cover slips were fixed with methanol at −20°C for 4 min, washed in PBS, preincubated with 5% normal goat serum containing 2% bovine serum albumin and 0.1% Triton™ X-100, and incubated with the monoclonal human antibodies starting at a 1:10 dilution overnight at 4°C. Sections were washed in PBS and coverslips mounted with Immu-Mount™ (ThermoScientific). Double-labelling of transfected cells was performed using commercial monoclonal mouse anti-NR1 antibodies (1:100, Synaptic Systems; generated against amino acids 660-811 of rat GluN1).

Immunohistochemistry

Rat and mouse brain sections were used as unfixed tissue or after paraformaldehyde fixation, cut on a cryostat in 15 µm sections and mounted on glass slides. Fixed tissue was permeabilized in 0.1% Triton™ X-100 in PBS for 20 min and blocked in 10% normal goat serum for 30 min, unfixed tissue was not permeabilized. Monoclonal human antibodies were diluted to 30 µg/ml and sections incubated overnight at 4°C, human CSF was used undiluted. Further stainings included rabbit polyclonal anti-NR1 (1:100, Synaptic Systems; generated

against amino acids 35-53 of rat GluN1), anti-MAP2 (1:500, Millipore).

Site-directed mutagenesis

Point mutation N368Q was introduced into the NR1 construct using the Stratagene QuikChange™ Mutagenesis kit according to manufacturer's instructions, and the mutant transiently transfected in HEK cells as described previously (Doss *et al.*, 2014).

Flow cytometry and epitope competition assay

Unfixed NR1-expressing HEK cells were incubated with monoclonal human antibodies (100 µg/ml) for 45 min, washed in PBS and incubated with an allophycocyanin-conjugated secondary anti-human antibody for 30 min. Median fluorescence intensity was measured using a FACSCanto™ II (BD Biosciences). For epitope competition, HEK cells were first incubated with commercial rabbit NR1 antibodies in increasing concentrations, washed, and incubated with human NR1 antibodies as above.

Primary hippocampal neurons

Brains from murine pups (postnatal Days 1–3) were transferred into Hanks balanced salt solution (HBSS) with 10 mM HEPES buffer (pH 7.3). For glial preparation, cortices were incubated at 37°C for 20 min with 0.5% trypsin/EDTA (TE) solution and transferred into astrocyte media (DMEM containing 0.45% glucose, 1000 U/ml penicillin, 1000 µg/ml streptomycin and 10% foetal bovine serum). Cortices were dissociated and grown in astrocyte media for 14 days. Astrocytes were trypsinated, washed and seeded with a density of 45 000 cells/well into 24-well plates to provide a glial feeding layer for neurons. Mitogenesis was stopped after 6 days by incubation for 24 h with 40.5 µM 5-fluoro-2-desoxyuridine and 102 µM uridine in DMEM. To condition the media for neuronal growth, astrocyte media was exchanged to neuron media (Neurobasal® Media A for postnatal neurons supplemented with 100 U/ml penicillin, 100 µg/ml streptomycin and 0.5 mM L-alanyl-L-glutamine) the day before preparation. For neuronal preparation, hippocampi were incubated with 2.5% trypsin at 37°C for 15 min, washed three times in HBSS and taken up in 500 µl neuron media. Hippocampi were dissociated with a fire-polished, narrowed glass pipette, cells counted and plated at 20–40 000 cells/well in neuron media on 12 mm poly-L-lysine (PLL)-treated coverslips. After 4–5 h, attached neurons were transferred upsid-down on the glial feeding layer and cultured for 7–21 days. Distance between the layers was kept by small dots of paraffin that were placed on the coverslips prior to PLL treatment.

NMDAR cluster downregulation

Hippocampal neurons were incubated with 0.5 µg/ml human monoclonal NR1 or control antibody at 37°C for 18 h. Cells were fixed with methanol and stained with rabbit polyclonal anti-NR1 (1:100, Synaptic Systems) as above. The control antibody (mGo53) is a non-reactive human antibody previously described (Wardemann *et al.*, 2003). For each condition, 94 neurons were selected from three independent experiments, and three dendrite sections of 50 µm lengths were counted per cell.

In vivo binding of monoclonal antibodies

Eight-week-old C57Bl/6 mice were intravenously injected with a single dose of 60 µg monoclonal NR1 or control antibody. After 24 h, mice were euthanized, brains removed, unfixed parasagittal sections cut on a cryostat and stained with an anti-human immunoglobulin secondary antibody.

Electrophysiological recordings

Cultured murine hippocampal neurons [days *in vitro* (DIV) 13–15] were incubated with recombinant antibodies for 18 h at 0.5 µg/ml. Cells were transferred to a submerged recording chamber continuously perfused with extracellular buffer containing 140 mM NaCl, 2.4 mM KCl, 10 mM HEPES, 10 mM glucose, 2 mM $CaCl_2$, and 1 mM $MgCl_2$, pH adjusted to 7.3 with NaOH, 300 mOsm at room temperature. MNI-caged-L-glutamate (Tocris) was added at a final concentration of 100 µM for glutamate uncaging experiments, which were performed in the presence of the NMDAR co-agonist glycine (10 µM, Sigma), the $GABA_BR$ antagonist SCH 50 911 (10 µM, Tocris), the $GABA_AR$ antagonist Gabazine (2 µM, Tocris), and the AMPAR antagonist NBQX (10 µM, Tocris) in order to isolate NMDAR-mediated currents. Whole-cell voltage clamp recordings were performed with borosilicate glass electrodes (2–5 MΩ) filled with 130 mM $KMSO_3$, 4 mM KCl, 10 mM HEPES, 4 mM Mg-ATP, 0.2 mM EGTA, 4 mM NaCl, 0.3 mM NaGTP, 10 mM phosphocreatine-Na_2; pH adjusted to 7.3 with KOH, 295 mOsm. Series resistance (Rs) was monitored continuously throughout experiments; cells were rejected if Rs was >25 MΩ or varied more than 30% during recordings. No Rs compensation was used. Photolysis of 'caged' glutamate was performed at 0.1 Hz with a 20 ms light pulse of a 355 nm DPSS laser system (Rapp Optoelectronics) coupled into the fluorescence light path of an Olympus BX-51 WI microscope, equipped with a 60×, 0.9 NA-objective, resulting in an effective light spot diameter of 15 µm in the focal plane, which was targeted directly on the soma of the neuron.

Calcium uptake

Hippocampal neurons were incubated with 15 µg/ml human monoclonal NR1 (clones 003-102 and 007-168 from Patients 2 and 4, respectively) or control antibody (mGo53) (Wardemann *et al.*, 2003) at 37°C for 18 h. The membrane permeant calcium sensitive dye Fluo-4 (Life Technologies) was dissolved at 4 mM in DMSO) and cells loaded with a 1:5000 dilution for 30 min at 37°C. Coverslips were rinsed in prewarmed HEPES-buffered Tyrode's solution (HBTS, 118 mM NaCl, 4.8 mM KCl, 2 mM HEPES, 2 mM $CaCl_2$, 2 mM $MgCl_2$, 33 mM Glucose), and transferred into wells containing 300 µl HBTS with 10 µM NBQX. Calcium influx across NMDAR was stimulated with injection of 200 µl NMDA solution to a final concentration of 10 µM with no wash-out

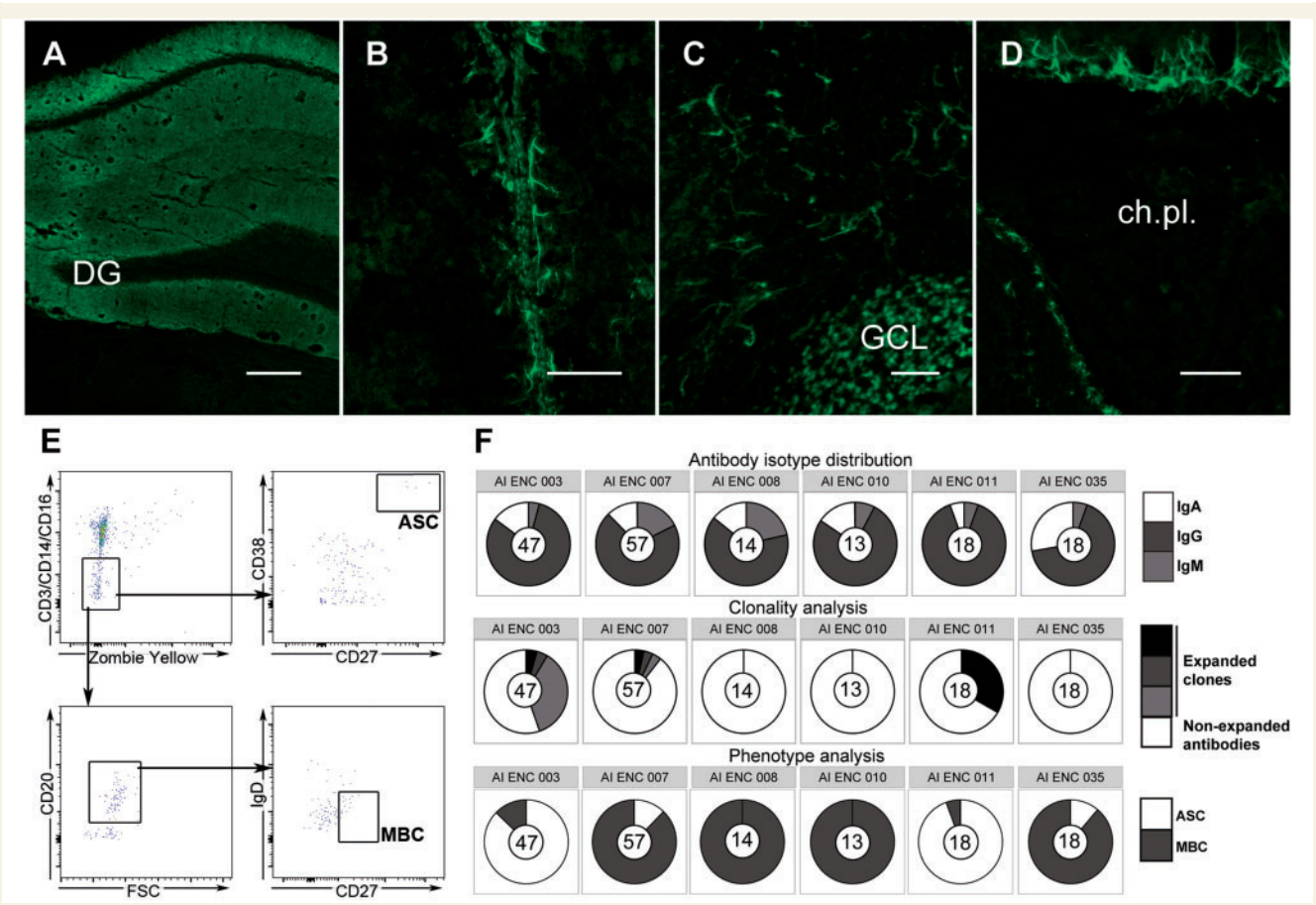

Figure 1 Antibody repertoire and clonality analysis in the CSF of patients with NMDAR encephalitis. Immunofluorescence on unfixed hippocampus sections using CSF from patients with NMDAR encephalitis shows characteristic antibody binding to neuropil (**A**), but commonly also to further epitopes that do not overlap with NMDAR expression, such as astrocytic elements along brain surfaces (**B**), in the deep cerebellar white matter (**C**) or around the ventricles (**D**). FACS sorting plots demonstrating the isolation of $CD38^+CD27^+$ antibody-secreting cells (ASC) and $CD20^+IgD^-CD27^+$ memory B-cells (MBC) (**E**). Recombinant monoclonal antibodies from these cells were mainly immunoglobulin G and included clonally expanded cells (**F**). Note that pie charts from six patients are presented as the number of generated antibodies from two further patients were too low for a meaningful clonality analysis. Scale bars: **A** = 200 μm; **B–D** = 100 μm. ch.pl. = choroid plexus; GCL = cerebellar granule cell layer; DG = dentate gyrus.

period. Live cell imaging was performed using an inverted fluorescence microscope (Olympus IX73) equipped with a complementary metal-oxide semiconductor (CMOS) camera (Zyla, Andor Technology) and LED illumination system (CoolLED, pE-100). A series of images was acquired at 800-ms intervals for 43.2 s at an excitation wavelength of 470 nm shortly before the stimulation to measure fluorescence intensity at resting Ca^{2+} levels and after the stimulation. The fluorescence intensity for each time point on the neuronal somata was measured using NIH ImageJ software and corrected for the baseline fluorescence measured before NMDA application.

Methods to prevent bias

Immunohistochemical quantification (NMDAR-containing clusters) and electrophysiological (NMDAR current amplitudes and calcium influx) recordings were performed blinded to the presence of either control or NR1 antibodies.

Statistics

Hippocampal culture experiments (cluster density, NMDAR currents and calcium influx) were analysed using two-tailed Mann Whitney U-test. Data are mean ± SEM. The accepted level of significance for all of the tests was $P < 0.05$.

Results

Only a small fraction of CSF B cells produce NMDAR antibodies

Immunofluorescence on brain sections using CSF from patients with NMDAR encephalitis shows characteristic antibody binding to hippocampus neuropil (Fig. 1A), but commonly also to further epitopes, such as astrocytic and neuronal elements, which do not overlap with NMDAR

Table 1 Sequence information of NR1-reactive antibodies

Event ID	Clone number	Phenotype	Isotype	IGHV	IGHD	IGHJ	IGH CDR3	IGHV SHM	Light chain	IGKV/IGLV	IGKJ/ IGLJ	IGK/IGLCDR3	IGKV/I GLV SHM	Clonal status
003-102	1	ASC	IgG1	4-4*02	2-15*01	5*02	ARDVSGGVNWFDP	4	Lambda	6-57*01	2*01	QSYDSSTVV	2	Non-expanded
003-109	2	ASC	IgG2	3-33*01	3-3*01	3*02	ARRHYDFDAFDI	0	Lambda	2-14*01	1*01	SSYTSSSTLYV	0	Non-expanded
007-142	3	ASC	IgG1	5-51*01	4-17*01	4*02	ARDYGDYYFDY	1[a]	Lambda	2-11*01	2*01	CSYAGSYTGV	0	Expanded
007-169		ASC	IgG2	5-51*01	4-17*01	4*02	ARDYGDYYFDY	1[a]	Lambda	2-11*01	2*01	CSYAGSYTGV	0	Expanded
007-124	4	ASC	IgG1	3-20*01	6-19*01	5*02	AREVGIAVTGYWFDP	8	Lambda	3-21*02	2*01	QVWDSSSDHPGVV	12	Expanded
007-176		ASC	IgG1	3-20*01	6-19*01	5*02	AREVGIAVTGYWFDP	8	Lambda	3-21*02	2*01	QVWDSSSDHPGVV	12	Expanded
007-157	5	MBC	IgG3	5-51*01	2-2*02	4*02	ARSAVFDY	10	Kappa	3-15*01	1*01	QQYNNWPTSWT	3	Expanded
007-168		MBC	IgG3	5-51*01	2-2*02	4*02	ARSAVFDY	10	Kappa	3-15*01	1*01	QQYNNWPTSWT	3	Expanded
008-218	6	MBC	IgG3	3-9*01	6-19*01	6*02	AKDRASSWYAYGMDV	4	Lambda	6-57*01	2*01	QSTRV	3	Non-expanded

V(D)J germline gene segments with highest sequence homology are listed for each heavy chain (IGH) and kappa (IGK) or lambda (IGL) light chain. For each Ig chain the amino acid sequence of the complementarity determining region 3 (CDR3) as well as the number of somatic hypermutations (SHM) in the V gene segment in comparison to the annotated germline sequences are shown. Expanded clones share complete identity for V(D)J gene segments for heavy and light chains and CDR3 mutation numbers and patterns.

[a]Silent mutation.

expression in six of eight patients in the present study (Fig. 1B–D). To characterize the broadness of the antibody repertoire expressed by CSF cells in patients with NMDAR encephalitis we isolated $CD27^+CD38^+$ antibody-secreting cells and $CD20^+IgD^-CD27^+$ memory B cells from CSF of eight consecutive patients using flow cytometric single cell sorting (Fig. 1E). All patients were diagnosed with NMDAR encephalitis based on the typical clinical picture, presence of CSF inflammation, and detection of NR1 autoantibodies in the CSF (Supplementary Table 1). The single purified antibody-secreting cells and memory B cells were then subjected to amplification, sequencing and cloning of their full-length immunoglobulin heavy (*IGH*) and corresponding immunoglobulin kappa (*IGK*) or lambda (*IGL*) light chain genes (Supplementary Tables 2 and 3). Sequence analysis confirmed that sorted cells were antigen-experienced B cells, and that the majority of antibody-secreting cells and memory B cells carried somatically mutated immunoglobulin genes and had undergone class-switching predominantly to immunoglobulin G (Fig. 1F). Immunoglobulin gene repertoire analysis showed no striking bias in V and J gene family usage or other antibody features compared to peripheral antibody-secreting cells and memory B cells as previously published (Tiller *et al.*, 2007) (Supplementary Fig. 1). Next we cloned the *IGH* and corresponding *IGK/IGL* variable genes into immunoglobulin G1 expression vectors to generate recombinant monoclonal antibodies. These were tested for reactivity against the NR1 subunit of the NMDAR expressed on HEK cells (Fig. 2A–D). Of 170 monoclonal antibodies from eight donors, we identified nine with reactivity to NR1 (three non-expanded, three expanded clones; Table 1), belonging to three patients. NR1-reactive clones were derived from two antibody-secreting cells in Patient 2 (acute encephalitis, 1 week from onset), four antibody-secreting cells and two memory B cells in Patient 4 (acute encephalitis, 6 weeks), and one memory B cell in Patient 5 (remission phase, 12 weeks) (Supplementary Table 3).

NMDAR reactivity was confirmed on murine primary hippocampal neurons (Fig. 2E, F and H–K), live cells (Fig. 2G) and rat and mouse brain sections (Fig. 2L and M). High-resolution double-labelling images showed largely overlapping patterns with a commercially available rabbit NR1 antibody (Fig. 2H–J). NMDAR clusters co-localized with the staining of VGLUT1, a marker for excitatory presynaptic terminals (Fig. 2K). On brain sections, human NR1 antibodies displayed a strong characteristic hippocampal neuropil staining (Fig. 2L) and typical staining of cerebellar granule cells (Fig. 2M). Intravenous injection of monoclonal antibodies into mice resulted in strong enrichment of NR1 (but not control) antibodies in the brain with high accumulation in the hippocampal neuropil (Fig. 2N) and cerebellar granule cells (Fig. 2P).

Interestingly, >95% of CSF-derived antibody-secreting cells and memory B cells that resulted in non-NMDAR-binding recombinant antibodies showed strong reactivity

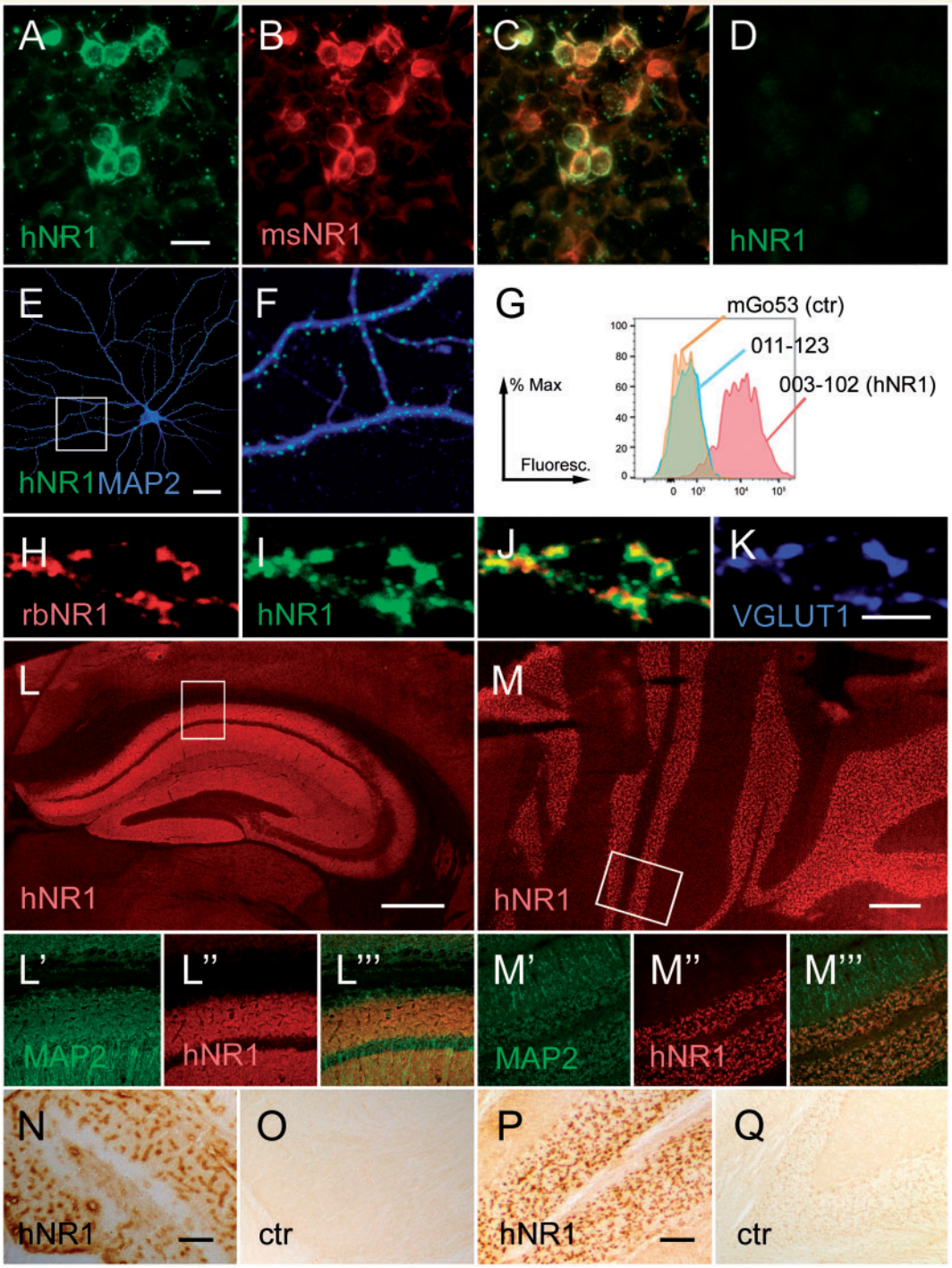

Figure 2 Identification of NR1-positive clones. All monoclonal human recombinant antibodies were screened for binding to NR1-transfected HEK cells (**A**). Positive staining was confirmed by double-labelling with a commercial anti-NR1 antibody (**B**), merged image in (**C**), and absence of staining on untransfected cells (**D**). Similar results were obtained on primary mouse hippocampal neurons (**E**, **F** and **H–K**). Double-labelling with MAP2 visualized the typical cluster distribution of NMDARs (**E**, higher magnification of the boxed area in **F**). Likewise, NR1 antibodies strongly bound to NR1-transfected live HEK cells using flow cytometry (**G**, red), while non-NR1 clones did not [**G**, e.g. 011-123 or control (ctr) antibody]. High resolution images demonstrated similar localization of a commercial NR1 antibody (**H**) with the monoclonal human antibodies (**I**, merged image in **J**) and VGLUT1, a marker of excitatory synaptic inputs (**K**). Monoclonal NR1 antibodies displayed the typical neuropil staining in rodent hippocampal (**L**) and cerebellar sections (**M**). Higher magnification of the boxed areas in **L–M** showing double-labelling with MAP2 (**L' M'**) and human NR1 (**L''**, **M''**), merged images (**L'''**, **M'''**). Antibody binding to *in vivo* epitopes in the mouse brain was demonstrated after intravenous injection, resulting in strong binding of NR1 antibodies to hippocampal neuropil (**N**) and cerebellar granule cells (**P**), not seen with control antibodies (**O** and **Q**). Scale bars: **A–D** = 25 μm; **E** = 20 μm; **H–K** = 4 μm; **L** and **M** = 500 μm; **N** and **O** = 200 μm; **P** and **Q** = 100 μm.

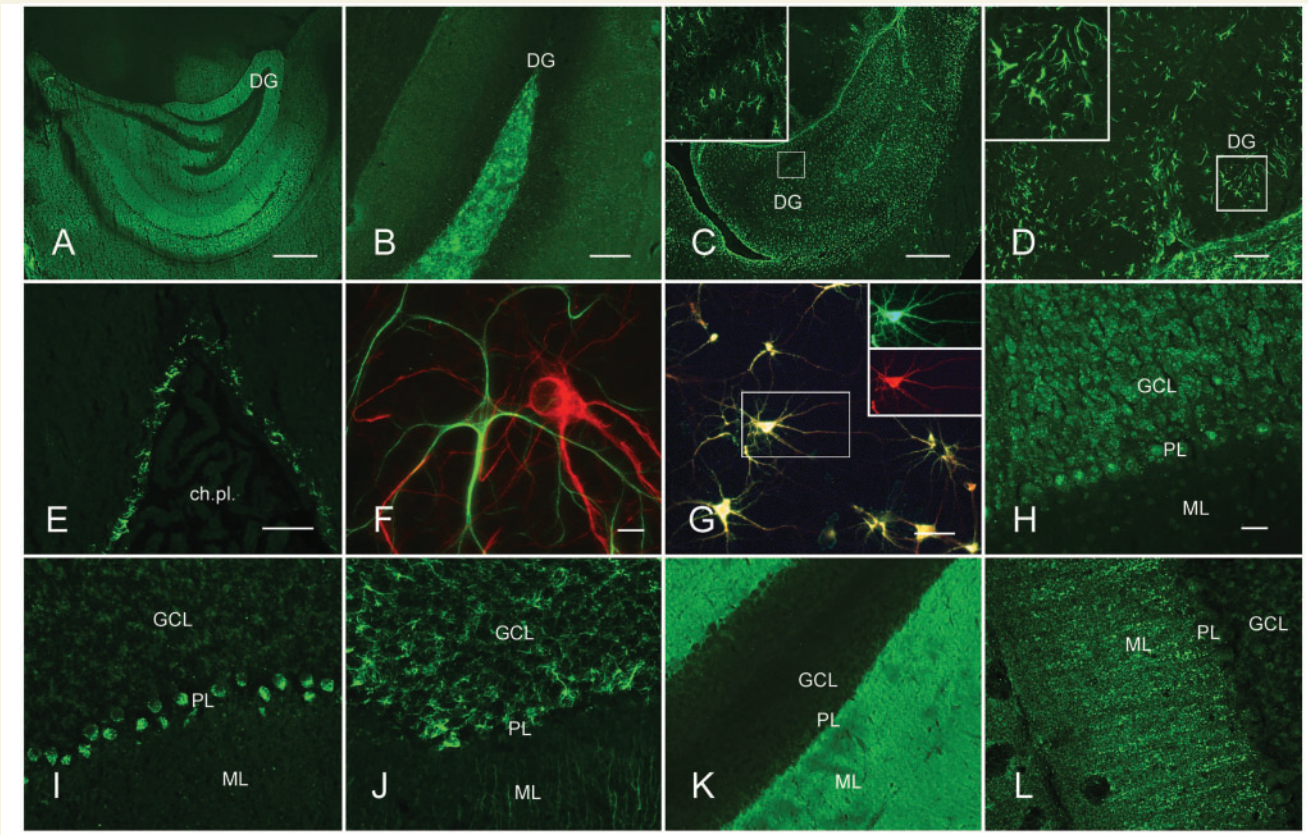

Figure 3 Immunohistochemistry of non-NR1-reactive monoclonal antibodies from the CSF of patients with NMDAR encephalitis. Several antibodies bound to hippocampus neuropil in a very similar (but not identical) pattern as NR1 antibodies, such as clone 003-165 (**A**). Others detected the endfolium area of the hippocampus, which is characteristically spared by NMDAR antibodies (**B**, 003-119). Clones from different patients showed strong binding to astrocytes, for example overlapping the NR1 distribution in the hippocampus (**C,** 011-116; **D,** 011-123; inserts show higher magnification of the boxed areas) or binding to the glia limitans along brain surfaces or the wall of the fourth ventricle (**E**, 011-146). Glial binding was confirmed in primary astrocyte cultures, exemplarily shown for clone 011-123 (**F**, green; MAP2 staining of a neuron in red). Tissue binding to neurons was confirmed in live primary hippocampal neurons (identified with MAP2), exemplarily shown for clone 003-165 (green) (merged in **G**). In the cerebellum, multiple antibodies specifically bound either granule cells (**H**, 010-330), Purkinje cell surfaces (**I**, 011-154), subtle networks around granule cells (**J**, 011-116), which are known to also highly express NR1 (*c.f.* Fig. 2M), or to the neuropil of the molecular layer in different intensities and patterns (**K**, 007-146; **L**, 003-104). Scale bars: **A** = 500 μm; **B** = 200 μm; **C–E** = 100 μm; **F** = 20 μm; **G–L** = 50 μm. ch.pl. = choroid plexus; DG = dentate gyrus; GCL = granule cell layer; PL = Purkinje cell layer; ML = molecular layer.

with further specific epitopes on brain sections, thus clearly outnumbering the NR1-reactive antibodies. The epitopes included endothelium, glial cells, neuronal surfaces of hippocampal granule cells, Purkinje neurons, or neuropil staining in cerebellum and hippocampus (Fig. 3).

Monoclonal NR1 antibodies can be unmutated and target a small epitope of the amino terminal receptor domain

Sequence analysis showed that the NMDAR antibodies were polyclonal immunoglobulins and often carried somatic hypermutations. However, we also identified germline NMDAR antibodies suggesting that the antibody-secreting cells had developed from unmutated naïve precursors (Supplementary Fig. 2). Several expanded clones were observed among NMDAR and non-NR1-reactive antibodies. Clonal members were identical in their somatic hypermutations pattern suggesting that diversification of the common ancestor happened before the cells proliferated. Binding of patients' antibodies to a small epitope of the amino-terminal domain of the NR1 subunit has been reported previously. We therefore generated an NR1 subunit construct with amino acid 368 mutated (N368Q) and tested the NR1-specific clones for their reactivity in transfected HEK cells. Indeed, binding to the mutant was eliminated for all monoclonal NR1 antibodies from different patients, including the germline-configured clones (Fig. 4C and F), while two commercial antibodies targeting different NR1 epitopes were still detected (Fig. 4B and E). Competition assays further confirmed that the commercial antibodies detected different

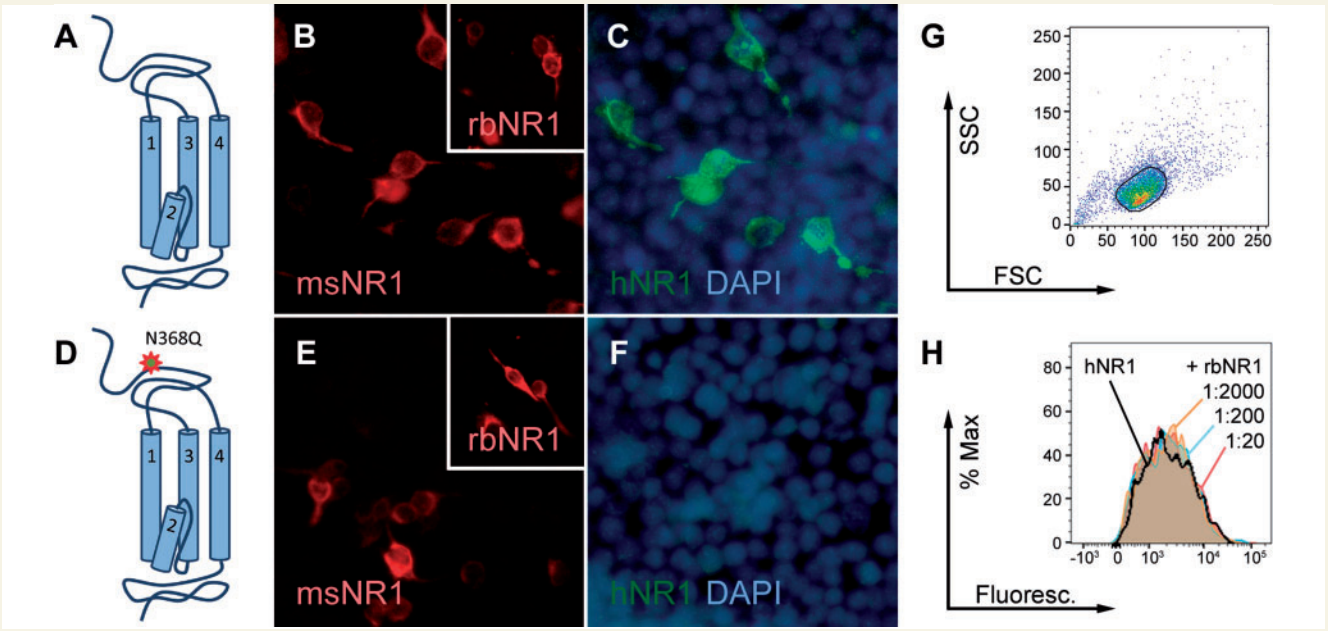

Figure 4 Epitope analysis of monoclonal human NR1 antibodies. HEK cells were transfected with wild-type NR1 (**A–C**) or a construct with amino acid 368 mutated (N368Q) (**D–F**). As exemplarily shown for clone 007-168, all human monoclonal NR1 (hNR1) antibodies strongly recognized NR1 (**C**), but staining of the mutant was eliminated (**F**). In contrast, a commercial mouse (msNR1) and rabbit anti-NR1 (rbNR1) antibody recognizing different NR1 epitopes bound to both wild-type (**B**) and N368Q (**E**). Staining of NR1-expressing HEK cells (**G**) with the monoclonal NR1 antibody resulted in high fluorescence intensity (**H**, black line). The signal was not reduced after preincubation with rabbit NR1 antibodies, further confirming the binding to different epitopes (**H**). FSC = forward scatter; SSC = side scatter.

epitopes as the human monoclonal NR1 antibodies (Fig. 4G and H).

Monoclonal NR1 antibodies disrupt synaptic NMDAR currents and morphology

To determine if NMDAR binding influenced neuronal cell function, we incubated primary murine hippocampal neurons with the purified monoclonal human NR1 or control antibody. Indeed, antibody-binding resulted in profound downregulation of NMDAR-positive synaptic clusters (Fig. 5A and B). Average cluster density was 8.4 per 50 µm dendrite length in the control group and 4.7 in the NR1 antibody-treated group, which represented a >45% reduction of NMDAR clusters (Fig. 5C) ($P < 0.0001$, Mann-Whitney U-test). We next examined whether the morphological changes after NR1 antibody treatment also lead to functional impairment in hippocampal neurons using whole cell patch clamp recordings. NMDAR-mediated currents were isolated in the presence of AMPA/kainate- and GABA receptor blockers. Laser-induced uncaging of glutamate triggered NMDAR-mediated currents of 220 ± 61 pA in control antibody-treated and 119 ± 15 pA in NR1 antibody-treated neurons (~46% reduction, Fig. 5D and E) ($P = 0.016$, Mann-Whitney U-test). In line with the electrophysiological observations, calcium imaging experiments using monoclonal NR1 antibodies from two different patients, revealed a profoundly reduced NMDA-induced calcium influx, affecting the total amount of calcium influx (area under the curve) as well as calcium peak concentration (Fig. 5F–H) ($P < 0.0001$, Mann-Whitney U-test).

Discussion

The present study provides data on the CSF antibody repertoire in NMDAR encephalitis and shows that binding of human monoclonal NR1 antibodies to NMDARs is sufficient to cause morphological and electrophysiological changes in neurons resulting from NMDAR downregulation. Thus, it provides ultimate proof that CSF-derived NR1 antibodies from patients with NMDAR encephalitis can solely cause these changes and that it did not depend on the presence of additional anti-neuronal antibodies, complement activation, or further undetermined molecules. It also provides evidence that seropositivity for the here described NMDAR autoantibodies must be considered a risk factor for neuropsychiatric symptoms (similar to a drug or toxin level), and supports the concept that CSF antibody titres are intraindividual disease biomarkers correlating with clinical remission (Gresa-Arribas *et al.*, 2014).

However, the present study demonstrated that NR1 antibody-producing cells are relatively rare in the CSF, making

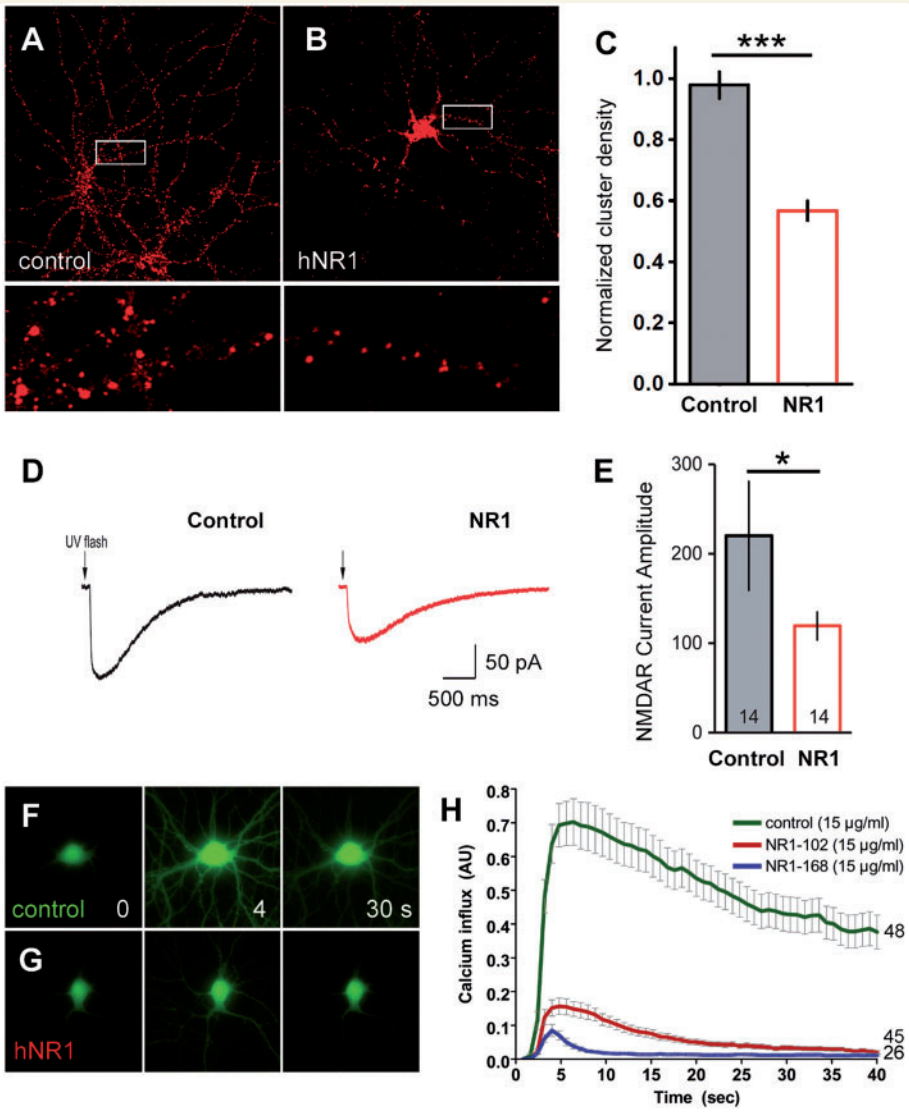

Figure 5 Monoclonal human NR1 antibodies downregulate NMDAR clusters and suppress channel function. Primary hippocampal neurons displayed characteristic NMDAR-containing clusters along their dendritic arborizations when stained with a rabbit anti-NR1 antibody. Cultures treated with control antibody for 18 h showed unchanged morphology (**A**, boxed area is enlarged in the *bottom panel*), while cultures treated with human monoclonal NR1 antibody showed profound loss of clusters (**B**). Quantification showed reduction of cluster density by $>45\%$ ($P < 0.0001$) (**C**). NMDAR currents were evoked by UV light-assisted glutamate uncaging on the soma of cultured hippocampal neurons (**D**). Glutamate uncaging-evoked currents were profoundly reduced in NR1 antibody-treated neurons ($P = 0.016$) (**E**). NMDAR function in hippocampal cultures was further evaluated by neuronal stimulation with 10 µM NMDA; representative video sequences demonstrate fluorescence intensity of the calcium-sensitive dye Fluo4 at 0, 4 and 30 s after stimulation when pretreated for 18 h with non-neuronal control antibody (**F**) or different human monoclonal NR1 antibodies (**G**). Quantification of calcium influx (arbitrary units) showed marked reduction in NR1 antibody-treated cultures ($P < 0.0001$) (**H**). Data are mean ± SEM from ⩾3 independent experiments, Mann-Whitney U-test. $n = 3 \times 50$ µm sections of 94 neurons (**C**), $n = 14$ for both groups (**D** and **E**), $n = 26$–48 neurons (**H**).

up only ~6% of antibody-secreting cells/memory B cells. This was surprising as most patients show intrathecal synthesis of NMDAR antibodies (Gresa-Arribas *et al.*, 2014) associated with the presence of large numbers of antibody-secreting cells that can exceed 10% of all CSF cells (Dale *et al.*, 2013), suggesting that a large proportion of antibody-secreting cells might be disease-specific producing NMDAR antibodies. Despite the low frequency, NR1 antibodies might reach high concentrations in the brain tissue as autopsy reports from the acute phase of the encephalitis demonstrated increased antibody-secreting cell numbers in the meninges and brain parenchyma (Martinez-Hernandez *et al.*, 2011).

Surprisingly, the vast majority of antibody-secreting cells/memory B cells produced antibodies that did not bind to NR1, but reacted against further brain-expressed epitopes including neuronal surface antigens in hippocampus and cerebellum. The finding suggests that these cells are

specifically enriched in the CNS in which their antigens are present. Clonal expansions were observed for both NR1- and non-NR1-reacting B cells. Extensive future work will have to elucidate the target protein specificity of non-NR1 antibodies, and will show whether these antibodies can also change morphology and electrophysiological properties of neuronal receptors, which seems possible given their neuropil and neuronal surface reactivity. Thus, they could potentially contribute to the highly variable clinical phenotype of NMDAR encephalitis, ranging from isolated psychosis to severe cognitive impairment, hypoventilation or brainstem dysfunction.

The here described molecular features of NR1 autoantibodies support the concept that ectopically expressed NMDAR protein (such as in ovarian teratomas) can trigger NMDAR encephalitis (Day *et al.*, 2014). Generally, highly autoreactive bone marrow-derived B cells are regulated at central and peripheral tolerance checkpoints (Wardemann *et al.*, 2003). The presence of NMDAR germline antibodies suggests that tolerance induction is incomplete or absent against the non-peripheral neuronal protein NMDAR. In the absence of access to the brain the presence of rare peripheral anti-NR1 B cells may not pose a risk. Expression of this otherwise non-accessible protein on the tumour may explain positive selection and expansion of high-affinity NR1-reactive B cells. Once these clonally expanded and affinity-matured cells get access to the brain, local antigen-mediated activation of anti-NMDAR naïve and pre-existing memory B cells may induce and fuel the disease progression.

In addition to previously reported immunoglobulin G1 and immunoglobulin G3 isotypes (Hughes *et al.*, 2010), immunoglobulin G2 NR1 antibodies can be part of the CSF repertoire. The surprisingly low number of somatic hypermutations in heavy and light chains (including even germline encoded antibodies), the finding that clonally expanded CSF B cells carried identical somatic hypermutations patterns, and the high NR1 antibody titres in serum suggest that these cells originated from peripheral immune responses rather than from clonal expansion and diversification in the CSF. NR1 antibodies were also cloned from persistent memory B cells suggesting that memory can be formed during encephalitis. Reactivation and differentiation into NR1-specific antibody-secreting cells may be associated with clinical relapses.

The recombinant human monoclonal antibodies will be useful tools for high resolution synaptic imaging and future research into the molecular mechanisms and clinical correlations in NMDAR encephalitis. Using the same methodology, monoclonal antibodies from patients with neuropsychiatric lupus (DeGiorgio *et al.*, 2001), monosymptomatic psychiatric NMDAR encephalitis (Deakin *et al.*, 2014), or NMDAR-immunoglobulin A antibody-associated cognitive decline (Prüss *et al.*, 2012; Doss *et al.*, 2014) will be equally examined for pathogenicity, thus uncovering disease mechanisms of diverse neuropsychiatric phenotypes related to NMDAR autoimmunity.

Acknowledgements

We gratefully acknowledge the help of Dr Frauke Ackermann and Carolin Gehr with calcium imaging experiments.

Funding

This study has been supported by grants from the German Academic Exchange Service (to H.P.; DAAD, D/10/43923), the German Research Foundation (DFG, to H.P.: PR 1274/2-1; DFG Exc257 NeuroCure to F.P., D.S., A.M. and AEH; DFG TRR130 P17 to A.E.H. and H.R.; DFG TRR84 to A.M.; DFG SFB958 to D.S.), Federal Ministry of Education and Research (BMBF smart-age, to D.S.), Focus Area DynAge (Freie Universität Berlin and Charité Berlin, to H.P.).

Supplementary material

Supplementary material is available at *Brain* online.

References

Corbett SJ, Tomlinson IM, Sonnhammer EL, Buck D, Winter G. Sequence of the human immunoglobulin diversity (D) segment locus: a systematic analysis provides no evidence for the use of DIR segments, inverted D segments, "minor" D segments or D-D recombination. J Mol Biol 1997; 270: 587–97.

Dale RC, Pillai S, Brilot F. Cerebrospinal fluid CD19(+) B-cell expansion in N-methyl-d-aspartate receptor encephalitis. Dev Med Child Neurol 2013; 55: 191–3.

Dalmau J, Tüzün E, Wu HY, Masjuan J, Rossi JE, Voloschin A, et al. Paraneoplastic anti-N-methyl-D-aspartate receptor encephalitis associated with ovarian teratoma. Ann Neurol 2007; 61: 25–36.

Day GS, Laiq S, Tang-Wai DF, Munoz DG. Abnormal neurons in teratomas in NMDAR encephalitis. JAMA Neurol 2014; 71: 717–24.

Deakin J, Lennox BR, Zandi MS. Antibodies to the N-methyl-D-aspartate receptor and other synaptic proteins in psychosis. Biol Psychiatry 2014; 75: 284–91.

DeGiorgio LA, Konstantinov KN, Lee SC, Hardin JA, Volpe BT, Diamond B. A subset of lupus anti-DNA antibodies cross-reacts with the NR2 glutamate receptor in systemic lupus erythematosus. Nat Med 2001; 7: 1189–93.

Doss S, Wandinger KP, Hyman BT, Panzer JA, Synofzik M, Dickerson B, et al. High prevalence of NMDA receptor IgA/IgM antibodies in different dementia types. Ann Clin Transl Neurol 2014; 1: 822–32.

Gleichman AJ, Spruce LA, Dalmau J, Seeholzer SH, Lynch DR. Anti-NMDA receptor encephalitis antibody binding is dependent on amino acid identity of a small region within the GluN1 amino terminal domain. J Neurosci 2012; 32: 11082–94.

Gresa-Arribas N, Titulaer MJ, Torrents A, Aguilar E, McCracken L, Leypoldt F, et al. Antibody titres at diagnosis and during follow-up of anti-NMDA receptor encephalitis: a retrospective study. Lancet Neurol 2014; 13: 167–77.

Hughes EG, Peng X, Gleichman AJ, Lai M, Zhou L, Tsou R, et al. Cellular and synaptic mechanisms of anti-NMDA receptor encephalitis. J Neurosci 2010; 30: 5866–75.

Kabat EA, Wu TT. Identical V region amino acid sequences and segments of sequences in antibodies of different specificities. Relative contributions of VH and VL genes, minigenes, and complementarity-determining regions to binding of antibody-combining sites. J Immunol 1991; 147: 1709–19.

Kabat EA, Wu TT, Perry HM, Gotteman KS, Foeller C. Sequences of proteins of immunological interest. Bethesda, MD: U.S. Dept. of Health and Human Services, Public Health Service, National Institutes of Health; 1983. 323 pp.

Kalev-Zylinska ML, Symes W, Young D, During MJ. Knockdown and overexpression of NR1 modulates NMDA receptor function. Mol Cell Neurosci 2009; 41: 383–96.

Martinez-Hernandez E, Horvath J, Shiloh-Malawsky Y, Sangha N, Martinez-Lage M, Dalmau J. Analysis of complement and plasma cells in the brain of patients with anti-NMDAR encephalitis. Neurology 2011; 77: 589–93.

Mikasova L, De Rossi P, Bouchet D, Georges F, Rogemond V, Didelot A, et al. Disrupted surface cross-talk between NMDA and Ephrin-B2 receptors in anti-NMDA encephalitis. Brain 2012; 135: 1606–21.

Moscato EH, Peng X, Jain A, Parsons TD, Dalmau J, Balice-Gordon RJ. Acute mechanisms underlying antibody effects in anti-N-methyl-D-aspartate receptor encephalitis. Ann Neurol 2014; 76: 108–19.

Peery HE, Day GS, Dunn S, Fritzler MJ, Prüss H, De Souza C, et al. Anti-NMDA receptor encephalitis. The disorder, the diagnosis and the immunobiology. Autoimmun Rev 2012; 11: 863–72.

Planaguma J, Leypoldt F, Mannara F, Gutierrez-Cuesta J, Martin-Garcia E, Aguilar E, et al. Human N-methyl D-aspartate receptor antibodies alter memory and behaviour in mice. Brain 2015; 138: 94–109.

Prüss H, Dalmau J, Harms L, Höltje M, Ahnert-Hilger G, Borowski K, et al. Retrospective analysis of NMDA receptor antibodies in encephalitis of unknown origin. Neurology 2010; 75: 1735–9.

Prüss H, Höltje M, Maier N, Gomez A, Buchert R, Harms L, et al. IgA NMDA receptor antibodies are markers of synaptic immunity in slow cognitive impairment. Neurology 2012; 78: 1743–53.

Prüss H, Leubner J, Wenke NK, Czirjak GA, Szentiks CA, Greenwood AD. Anti-NMDA Receptor Encephalitis in the Polar Bear (Ursus maritimus) Knut. Sci Rep 2015; 5: 12805.

Tiller T, Meffre E, Yurasov S, Tsuiji M, Nussenzweig MC, Wardemann H. Efficient generation of monoclonal antibodies from single human B cells by single cell RT-PCR and expression vector cloning. J Immunol Methods 2008; 329: 112–24.

Tiller T, Tsuiji M, Yurasov S, Velinzon K, Nussenzweig MC, Wardemann H. Autoreactivity in human IgG+ memory B cells. Immunity 2007; 26: 205–13.

Titulaer MJ, McCracken L, Gabilondo I, Armangue T, Glaser C, Iizuka T, et al. Treatment and prognostic factors for long-term outcome in patients with anti-NMDA receptor encephalitis: an observational cohort study. Lancet Neurol 2013; 12: 157–65.

Wardemann H, Yurasov S, Schaefer A, Young JW, Meffre E, Nussenzweig MC. Predominant autoantibody production by early human B cell precursors. Science 2003; 301: 1374–7.

Wasterlain CG, Naylor DE, Liu H, Niquet J, Baldwin R. Trafficking of NMDA receptors during status epilepticus: therapeutic implications. Epilepsia 2013; 54 (Suppl 6): 78–80.

Wright S, Hashemi K, Stasiak L, Bartram J, Lang B, Vincent A, et al. Epileptogenic effects of NMDAR antibodies in a passive transfer mouse model. Brain 2015; 138: 3159–67.